

# Winkler spring behavior in FE analyses of dowel action in statically loaded RC cracks

Diogo Figueira\*, Carlos Sousa<sup>a</sup> and Afonso Serra Neves<sup>b</sup>

CONSTRUCT-LABEST, Faculty of Engineering (FEUP), University of Porto, Portugal

(Received October 11, 2017, Revised February 13, 2018, Accepted February 25, 2018)

**Abstract.** A nonlinear finite element modeling approach is developed to assess the behavior of a dowel bar embedded on a single concrete block substrate, subjected to monotonic loading. In this approach, a discrete representation of the steel reinforcing bar is considered, using beam finite elements with nonlinear material behavior. The bar is connected to the concrete embedment through nonlinear Winkler spring elements. This modeling approach can only be used if a new constitutive model is developed for the spring elements, to simulate the deformability and strength of the concrete substrate. To define this constitutive model, an extensive literature review was conducted, as well as 3 experimental tests, in order to select the experimental data which can be used in the calibration of the model. Based on this data, an empirical model was established to predict the global dowel response, for a wide range of bar diameters and concrete strengths. This empirical model provided the information needed for calibration of the nonlinear Winkler spring model, valid for dowel displacements up to 4 mm. This new constitutive model is composed by 5 stages, in order to reproduce the concrete substrate response.

**Keywords:** dowel; reinforced concrete; shear transfer; structural analysis; finite element method; stiffness

## 1. Introduction

Cracking is normal and admitted in most reinforced concrete structures. However, crack widths have to be controlled so that the structure serviceability, durability and strength is not impaired. The structural behavior after cracking has to be analyzed and the required amount of steel reinforcement has to be determined. It has to be ensured that the applied efforts (namely shear and tension) can be transferred across the cracks and the structure deformability is kept within admissible limits. In this context, modeling of stress transfer across cracks in reinforced concrete is a difficult problem, mainly due to the complexity of the shear strength mechanisms involved and their numerical simulation (Dias-da-Costa *et al.* 2012, Kazaz 2011, Pimentel *et al.* 2008). The shear force,  $V$ , transferred through a crack, either in monolithic concrete or in a concrete joint, is mainly carried by two different mechanisms (Maekawa and Qureshi 1997, Rahal *et al.* 2016, Santos and Júlio 2014)

$$V = V_{agg} + V_d \quad (1)$$

in which  $V_{agg}$  is the force corresponding to aggregate interlock mechanism and  $V_d$  the dowel force of steel reinforcing bars.

This present paper focuses only on the contribution of dowel action. The strength of a dowel submitted to monotonically increasing load,  $V_{dR}$ , has been widely evaluated in several research studies (Bennett and Banerjee 1976, Dei Poli *et al.* 1992, Dulacska 1972, Engström 1990, Millard and Johnson 1984, Paulay *et al.* 1974, Randl 1997, Rasmussen 1963, Soroushian *et al.* 1986, Tanaka and Murakoshi 2011, Vintzeleou and Tassios 1987). This strength is usually predicted through the following analytical expression, whose background theory can be consulted in *fib* Bulletin 43 (2008)

$$V_{dR} = K \times A_s \times \sqrt{f_c \times f_y} \quad (2)$$

where  $A_s$  is the area of reinforcement,  $f_c$  the concrete compressive strength and  $f_y$  the reinforcement yield stress.  $K$  is an empirical constant that depends on the actual confinement existing in the concrete substrate immediately under the dowel bar

$$K = \frac{4}{\pi} \times \sqrt{\frac{\beta^*}{3}} \quad (3)$$

with

$$\beta^* = \frac{f_c^*}{f_c} \quad (4)$$

in which  $f_c^*$  is the concrete strength under a biaxial or triaxial stress state caused by confinement due to local compression. Regarding the coefficient  $K$ , Randl (2013) reviewed in a recent work the dowel strength experimental data available in literature. He concluded that  $K=1.5$  agreed the results collected with a rather low scatter. According to *fib* Model Code (2013),  $K$  should be less than 1.6. It is

\*Corresponding author, Ph.D.

E-mail: dec09012@fe.up.pt

<sup>a</sup>Assistant Professor

E-mail: cfsousa@fe.up.pt

<sup>b</sup>Associate Professor

E-mail: asneves@fe.up.pt

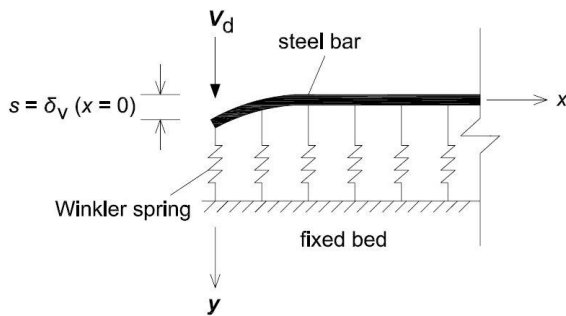


Fig. 1 Dowel action of a steel reinforcing bar modeled by the Beam resting on an Elastic Foundation analogy

important to note that the subscript  $d$  in the variable name  $V_{dR}$  does not mean “design value affected by partial safety factors”. This subscript means “dowel”. In this paper, Eq. (2) gives the predicted value for the real dowel strength.

Research studies devoted to modeling of dowel action nonlinear behavior are scarcer. Even though some empirical formulations have been proposed (Dulacska 1972, Millard and Johnson 1984, Vintzeleou and Tassios 1986, Walraven and Reinhardt 1981), modeling of the dowel force – slip ( $V_d-s$ ) relation is generally based on the Beam resting on an Elastic Foundation (BEF) analogy (Friberg 1938, Guo *et al.* 1995), see Fig. 1. In this context, Soroushian *et al.* (1987) performed tests to assess the elastic stiffness of the Winkler springs corresponding to concrete substrate under the steel bar. The results were the bases for the Dei Poli *et al.* (1992) nonlinear dowel action behavior proposal, which included a nonlinear coefficient  $\omega$  multiplying the concrete substrate elastic stiffness in the BEF expressions. Later, Maekawa and Qureshi (1996) developed an analytical model for reinforcing bars under combined axial pullout and transverse displacement. The model includes the effects of bar plasticity and combined axial and shear loading through a damage build-up parameter  $DI$ .

Finite element (FE) modeling of dowel action was implemented by Davids and Turkiyyah (1997) through a linear elastic 3D model composed of circular section steel beam elements and concrete regular solid brick embedment elements. Nodes corresponding to the contact area between the two materials had identical displacements. The authors described their approach as an embedded and discrete FE representation of the dowel mechanism. An improved proposal, with plasticity added through a perfect plastic branch in dowel behavior, was published by He and Kwan (2001). In this model, a smeared representation of dowel action is used, in which the effect of reinforcement is spread over the continuum concrete elements. The procedure consists on the direct assemblage of reinforcement dowel stiffness matrix into the stiffness matrices of adjoining concrete elements.

Later, more complex and realistic dowel action modeling was established by Kwan and Ng (2013). To estimate the behavior of a reinforcing bar subjected to both axial and transverse forces, the authors modeled the steel bar as a beam attached to the concrete substrate through interface elements simulating both dowel and bond-slip mechanisms. However, dowel action is considered in the

same way as in a smeared representation. Therefore, steel bar elements have no flexural stiffness and no rotational degrees of freedom.

Recently, FE approaches (Magliulo *et al.* 2014, Zoubek *et al.* 2014) comprising an embedded and discrete representation of dowel action, similar to the Davids and Turkiyyah (1997) model, have been carried out. The main upgrade of these new approaches relies on the fact that material plasticity is included in the bar and the elements simulating the concrete embedment. Bond slip is accounted for in the tangential direction of the reinforcing bar through interface elements. In the normal direction, a perfect steel/concrete adhesion is assumed. In this context, a recent improvement was implemented by Mackiewicz (2015), in which the interaction between the steel bar and the concrete substrate is modeled through interface gap elements.

Lately, the state-of-art of dowel action modeling for FE analysis is developing at a faster pace comparing to the previous years. This evolution path can be explained by a few factors. In experimental testing, it is difficult to design a setup that can isolate dowel mechanism so it can be the only shear transfer component (Moradi *et al.* 2012). Additionally, in terms of numerical modeling, a realistic analysis of dowel action implies a discrete representation with material plasticity included. This type of analysis is complex and time-consuming. Nevertheless, discrete modeling of dowel action is essential to investigate, for example:

- the reinforcement stresses, displacements and curvatures throughout the length of the bar;
- the dowel force for which a plastic hinge is formed in the steel bar, and the position of the hinge relative to the crack section;
- the amount of shear force transferred through kinking of the dowel reinforcement;
- the relative contribution of dowel action and aggregate interlock as a function of crack opening and sliding values.

The objective of this paper is to develop a modeling approach that can be a discrete representation of a reinforcing bar dowel action, to be used in those types of applications and analyses. Comparing with other works available in literature, the main achievement of this approach is the inclusion of nonlinear interface Winkler spring FEs simulating the local compression and the confinement conditions of the concrete substrate right under the steel bar. To that end, the paper presents an exhaustive literature review on experimental data which can be used for model calibration. New experimental test results are also shown. Then, an empirical model to describe the  $V_d-s$  relationship is proposed. This model is a modified version of the one originally developed by Dei Poli *et al.* (1992). After that, the constitutive model for the nonlinear Winkler springs is presented and calibrated. That constitutive model can be directly used in the FE analysis of an isolated steel bar dowel, this being the so called Fixed Bed approach. Finally, a different analysis approach is presented, in which the dowel bar is embedded in a continuum of linear elastic, solid or plane, FEs. This is the designated Embedded Dowel approach.



(a) Formwork and reinforcement



(b) Test setup

Fig. 2 Dowel specimens tested (DM1, DM2 and DM3)

## 2. Review and selection of experimental data

In this section, a literature review is carried out in order to collect the available experimental data concerning dowel strength assessment. Then, the data is scrutinized and interpreted, with the aim to arrive at conclusions that can sustain the choice of the tests suitable to be used in the calibration of the FE analysis methodology introduced in this paper.

### 2.1 Literature review on dowel strength experimental assessment

An extensive literature review allowed to identify 9 publications (Bennett and Banerjee 1976, Dei Poli *et al.* 1992, Millard and Johnson 1984, Paulay *et al.* 1974, Randl 1997, Rasmussen 1963, Soroushian *et al.* 1986, Tanaka and Murakoshi 2011, Vintzeleou and Tassios 1987) with experimental tests aiming to assess the monotonic strength of a steel dowel embedded in concrete.

Three tests (DM1, DM2 and DM3) performed on the present work are also included (see Fig. 2). This new campaign represents an attempt to remove aggregate interlock and isolate the dowel mechanism of the specimens tested by Figueira *et al.* (2015). Therefore, the same geometry, reinforcement, test setup and loading are considered. The difference with respect to the Figueira *et al.* (2015) specimens (M1, M2 and M3) consists on the placement of 2 brass sheets, 0.3 mm thick, on the shear plane between the concretes of different age, in a similar procedure to Dulacska (1972) and Soroushian *et al.* (1986) works. Values for  $f_c$  measured in cylinder specimens (0.30 m high and 0.15 m diameter) were 87.4 MPa and 31.5 MPa

for the concrete of the first and second casting stages of each specimen, respectively.

Table 1 presents the data collected. In this context, some notes are relevant:

- All tests considered were performed in reinforcing bars acting against concrete core and not against concrete cover.
- The value of  $f_c$  corresponds by default to the concrete compressive strength measured in cylinder specimens. For the publications where only cube specimens were tested, it is adopted  $f_c = 0.85 \times f_{cc}$ , where  $f_{cc}$  is the concrete compressive strength measured in cube specimens. In tests on specimens with two concretes cast at different times, the average compressive strength was considered.
- Dowel behavior depends on the angle between reinforcement axis and the shear plane, particularly due to different confinement conditions in the concrete substrate. In specimens with reinforcement axis not perpendicular to the shear plane, the dowel strength calculation should follow recommendations presented on Dulacska (1972), and Eq. (2) is not applicable to predict the strength of such specimens. For that reason, specimens with reinforcement axis not perpendicular to the shear plane were not accounted.
- In cases where the reinforcement yield stress was not measured,  $f_y$  is taken as the specified characteristic yield stress value.
- $s_1$  is the dowel displacement, at the reinforcement section where load is applied ( $\delta_v(x=0)$  of Fig. 1), when maximum force  $V_R$  is reached. In turn,  $s_{max}$  is the maximum dowel displacement measured in the test. In some published results,  $s$  values are not shown.
- $c$  is the lateral cover length (measured in the direction perpendicular to the line of action of the applied load  $V_d$ ) and  $\phi$  is the bar diameter.
- Single sided dowels correspond to specimens in which the reinforcing bar is embedded on a single concrete block. In double sided dowels, the reinforcing bar is embedded on two concrete blocks and dowel action is mobilized with the relative slipping between the blocks.

### 2.2 Selection of experimental data for model calibration

By comparing values calculated for coefficient  $K$ , based on the data provided by the different publications (see Table 2, where  $\mu$  is the average value and  $\sigma$  the standard deviation), a significant scatter can be observed. For a better understanding of the reasons behind the scatter, some aspects concerning the tests performed should be analyzed and compared, such as: specimen geometry, its reinforcement and the test setup. These features and parameters can give information about the presence of other phenomena besides dowel action, like concrete splitting and the aggregate interlock mechanism, which affect the force  $V_R$  measured in the test. Moreover, the influence on dowel behavior of the reinforcement kinking effect and the confinement imposed by stirrups can also be deciphered.

Concrete splitting cracks were identified by Vintzeleou and Tassios (1987) in the 4 specimens with concrete cover

Table 1 Dowel strength experimental data collected from literature review

test	$\phi$ (mm)	$f_c$ (MPa)	$f_y$ (MPa)	$V_R$ (kN)	$K$	$s_1$ (mm)	$s_{max}$ (mm)	$c / \phi$	dowel sides
Bennett and Banerjee (1976)									
2-6-1	6.4	44	410	6.88	1.59	-	-	stirrups	2
2-6-2	6.4	44	410	8.33	1.93	-	-	stirrups	2
2-6-3	6.4	44	410	10.60	2.45	-	-	stirrups	2
4-6	6.4	44	410	6.84	1.58	-	-	stirrups	2
2-13-1	12.7	44	410	22.55	1.33	-	-	stirrups	2
2-13-2	12.7	44	410	23.73	1.39	-	-	stirrups	2
2-13-3	12.7	44	410	27.26	1.60	-	-	stirrups	2
2-16	15.9	44	410	39.76	1.49	-	-	stirrups	2
2-19	19	44	410	43.75	1.15	-	-	stirrups	2
Dei Poli <i>et al.</i> (1992)									
A1	24	29.5	500	76.19	1.39	2.155	3.000	4.5	1
A2	24	29.5	500	80.00	1.46	2.990	2.990	4.5	1
A4	18	29.5	500	46.39	1.50	1.131	2.495	6.2	1
A6	18	29.5	500	49.42	1.60	2.120	2.373	6.2	1
A12	18	29.5	500	36.38	1.18	2.080	2.505	6.2	1
A13	18	29.5	500	45.09	1.46	2.046	2.540	6.2	1
A8	14	29.5	500	31.11	1.66	1.088	1.738	8.1	1
A9	14	29.5	500	27.24	1.46	1.429	1.995	8.1	1
A3	24	32.3	500	80.33	1.40	4.213	4.678	4.5	1
B1	24	32.3	500	84.08	1.46	4.951	5.188	4.5	1
B4	24	32.3	500	79.68	1.39	4.164	4.648	4.5	1
A10	18	32.3	500	46.25	1.43	3.441	3.622	6.2	1
B2	18	32.3	500	46.57	1.44	4.491	4.491	6.2	1
B5	18	32.3	500	43.46	1.34	4.092	4.509	6.2	1
B3	14	32.3	500	27.35	1.40	1.414	4.106	8.1	1
B6	14	32.3	500	27.02	1.38	2.728	4.261	8.1	1
E1	24	72.0	500	119.14	1.39	1.052	5.009	4.5	1
E2	18	72.0	500	75.96	1.57	0.829	4.859	6.2	1
E3	14	72.0	500	50.43	1.73	1.041	5.008	8.1	1
Figueira <i>et al.</i>									
DM1	8	59.5	605	19.57	2.05	5.007	5.007	3.6	2
DM2	8	59.5	605	17.82	1.87	1.054	4.993	3.6	2
DM3	8	59.5	605	15.82	1.66	1.315	4.986	3.6	2
Millard and Johnson (1984)									
21L	12	32.0	435	22.65	1.70	1.448	1.761	-	2
22L	12	32.7	435	20.55	1.52	1.551	1.752	-	2
23L	12	45.9	435	23.85	1.49	1.254	1.583	-	2
24L	16	23.5	435	32.40	1.60	1.716	1.764	-	2
Paulay <i>et al.</i> (1974)									
TA	6.35	24.95	317	6.00	2.13	2.211	2.411	stirrups	2
TB	9.53	24.95	317	11.70	1.85	2.496	2.496	stirrups	2
TC	12.7	24.95	317	19.20	1.70	2.500	2.500	stirrups	2
Randl (1997)									
55	6	41.7	653	7.70	1.65	1.090	19	stirrups	2
56	12	41.7	600	28.70	1.60	1.860	19	stirrups	2
57	12	41.7	600	34.30	1.92	2.330	19	stirrups	2
58	20	41.7	524	82.90	1.79	3.020	19	stirrups	2
59	12	41.7	600	39.85	2.23	2.380	19	stirrups	2
60	12	41.7	600	36.20	2.02	2.000	19	stirrups	2
61	12	41.7	600	40.33	2.25	2.100	19	stirrups	2
62	6	41.7	653	8.10	1.74	1.100	19	stirrups	2
63	12	41.7	600	34.60	1.93	2.260	19	stirrups	2
64	20	41.7	524	79.90	1.72	3.090	19	stirrups	2
81	6	18.3	653	6.00	1.94	1.610	19	stirrups	2
82	12	18.3	600	22.40	1.89	2.640	19	stirrups	2
83	20	18.3	524	58.10	1.89	3.230	19	stirrups	2

Table 1 Continued

test	$\phi$ (mm)	$f_c$ (MPa)	$f_y$ (MPa)	$V_R$ (kN)	$K$	$s_1$ (mm)	$s_{max}$ (mm)	$c/\phi$	dowel sides
Rasmussen (1963)									
D1	15.8	11.0	242	16.48	1.63	-	-	stirrups	1
D2	15.8	20.1	242	23.54	1.72	-	-	stirrups	1
D3	15.8	30.5	242	28.94	1.72	-	-	stirrups	1
D4	15.8	43.4	242	31.20	1.55	-	-	stirrups	1
D5	25.1	10.7	221	37.77	1.57	-	-	stirrups	1
D6	25.1	26.6	221	61.31	1.62	-	-	stirrups	1
D7	25.1	28.7	221	68.18	1.73	-	-	stirrups	1
D8	25.1	43.0	221	77.70	1.61	-	-	stirrups	1
D9	16	16.9	431	34.83	2.03	-	-	stirrups	1
D10	25.9	18.4	400	69.16	1.53	-	-	stirrups	1
Soroushian <i>et al.</i> (1986)									
T4	12.7	42.8	414	41.99	2.49	5.156	10.08	5.4	2
T6	19.05	42.8	414	59.95	1.58	1.549	8.585	3.4	2
T8	25.4	42.8	414	71.17	1.06	1.981	10.16	2.5	2
Tanaka and Murakoshi (2011)									
N2419	19.1	24.5	342	33.30	1.27	-	-	6.0	1
N3010	9.53	33.8	355	9.05	1.16	-	-	12.6	1
N3013	12.7	31.2	338	16.10	1.24	-	-	9.3	1
N3016	15.9	32.8	345	29.05	1.38	-	-	7.4	1
N3019	19.1	33.3	342	40.80	1.33	-	-	6.0	1
N30-345	19.1	33.3	374	39.35	1.23	-	-	6.0	1
N30-390	19.1	33.3	445	41.90	1.20	-	-	6.0	1
N4019	19.1	45.8	342	46.45	1.30	-	-	6.0	1
N5010	9.53	59.2	355	12.00	1.16	-	-	12.6	1
N5013	12.7	59.2	338	20.95	1.17	-	-	9.3	1
N5016	15.9	59.2	345	33.85	1.19	-	-	7.4	1
N5019	19.1	59.1	342	49.00	1.20	-	-	6.0	1
N50-345	19.1	59.1	374	52.85	1.24	-	-	6.0	1
N50-390	19.1	59.1	445	59.20	1.27	-	-	6.0	1
Vintzeleou and Tassios (1987)									
150,14-1	14	32	420	30.43	1.71	4	4	2.9	2
150,14-2	14	32	420	31.22	1.75	4	4	2.9	2
150,14-1	14	45	420	35.70	1.69	4	4	2.9	2
150,14-2	14	45	420	36.66	1.73	4	4	2.9	2

Table 2 Average values and standard deviation of the coefficient  $K$  obtained from the experimental data

tests	$n$	$K$		concrete splitting	aggregate interlock	kinking effect	confined by stirrups
		$\mu$	$\sigma$				
Bennett and Banerjee (1976)	9	1.61	0.38	no	unknown	yes	yes
Dei Poli <i>et al.</i> (1992)	19	1.45	0.12	no	no	no	no
Figueira <i>et al.</i>	3	1.86	0.20	yes	yes	yes	no
Millard and Johnson (1984)	4	1.58	0.09	unknown	unknown	yes	unknown
Paulay <i>et al.</i> (1974)	3	1.89	0.22	no	yes	yes	yes
Randl (1997)	13	1.89	0.20	no	yes	yes	yes
Rasmussen (1963)	10	1.67	0.15	no	no	no	yes
Soroushian <i>et al.</i> (1988)	3	1.71	0.73	yes	unknown	yes	no
Tanaka and Murakoshi (2011)	14	1.24	0.07	no	no	no	no
Vintzeleou and Tassios (1987)	4	1.72	0.03	yes	unknown	yes	no

of 40 mm. Moreover, specimen A1 of the Dei Poli *et al.* (1992) program, and tests T6 and T8 of Soroushian *et al.* (1986), revealed a sudden decrease in strength, which suggests that splitting failure occurred. Concrete strength and cover length are the main factors affecting splitting. This phenomenon was also noticed in 2 of the tests (DM2

and DM3) performed on the present work. The test results for the imposed dowel displacement  $s$  are shown in Fig. 3, as a function of dowel force  $V_d$  and crack opening  $w$ , respectively. In these figures,  $s$  is the sum of the slip in the two sides of the dowel. The outlook of specimen DM3 after testing showed wide spread cover detachment of the

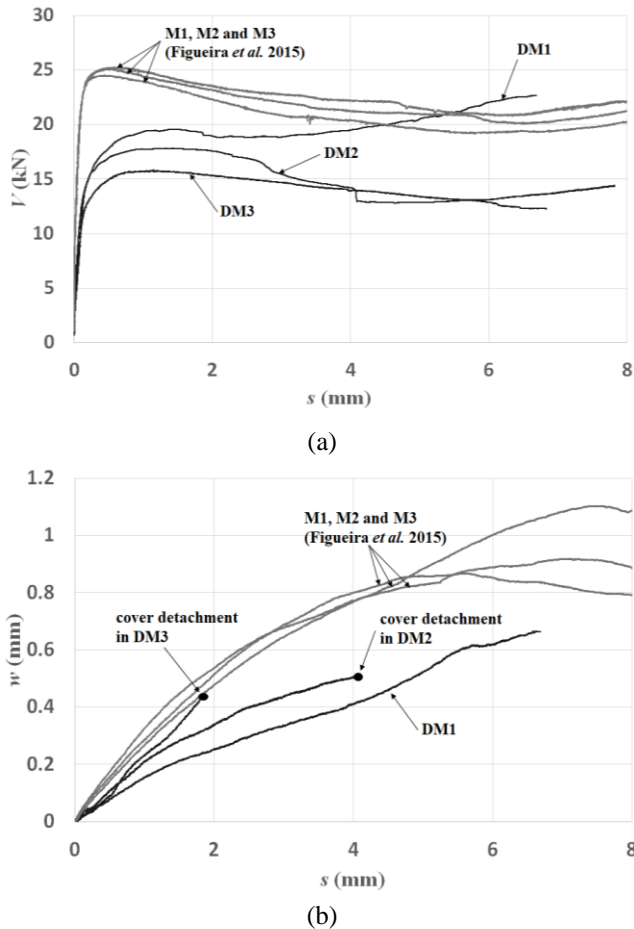


Fig. 3 Response obtained for the tested specimens: (a) force-displacement; (b) crack opening-displacement

concrete surrounding reinforcement. Specimen DM2 revealed a similar outlook comparing to DM3, also with clear cover detachment. On the other hand, the outlook of specimen DM1 did not disclose any significant superficial cracking, and consequently higher shear strength was achieved.

In Fig. 3(b), it can be seen that the crack opening behavior was not the expected for a test without friction at the interface between different concretes. Ideally, in a dowel test with very low friction, crack opening should be minimal. However, the values achieved were significant and not far from the ones relating to tests with interface friction (M1, M2 and M3). This behavior indicates that the execution procedure implemented in the dowel specimens was not totally effective to eliminate roughness in the interface between concretes. Therefore, besides reinforcement dowel action, aggregate interlock mechanism was also present, increasing shear strength.

Another phenomenon influencing dowel behavior can be plainly identified in specimen DM1 for large displacement values, in this case continuously amplifying shear strength. In double sided dowels, in which the reinforcing bar connects two concrete blocks, both slip and crack opening induce axial stress in the bar. With slip developing, the reinforcement axis exhibits an important rotation, in the position where the reinforcement intersects

the interface. As a consequence of this rotation, the reinforcement axial force grows the contribution to shear strength, a mechanism typically denoted as kinking or geometric effect of the dowel. This effect can also be found in specimens M1, M2 and M3. In tests with concrete splitting, DM2 and DM3, the strength increase caused by kinking is not so clear.

Even though the tests DM1 to DM3 were not well succeeded in terms of elimination of aggregate interlock effect, their results were shown here to demonstrate that other test results shown in the bibliography (using similar test procedures, with similar results) are also affected by interlock effects. Concrete splitting and reinforcement kinking can also be present in some of those works. For these reasons, certain criteria should be established in order to select experimental data that can be used in the calibration of a FE model for the dowel mechanism.

Aggregate interlock between concretes does not exist and the kinking effect is greatly minimized in tests performed on single sided dowels. Tests having these characteristics are the ones of Dei Poli *et al.* (1992), Rasmussen (1963), Tanaka and Murakoshi (2011). These three experimental campaigns have a significant number of specimens and no signs of concrete splitting, with the exception of Dei Poli *et al.* (1992) A1 test. However, even for this specimen, 1 out of 19, the value obtained for coefficient  $K$  was 1.39, therefore within the standard deviation of the sample.

Differences in dowel strength values between these three campaigns can be explained by a few factors. In Rasmussen (1963) campaign, concrete substrate is more confined since all specimens were reinforced with stirrups. And it is expected that a different amount of stirrups could lead to a variation in dowel strength. Dei Poli *et al.* (1992) specimens do not have stirrups and are made with a notch, so that the applied dowel force is aligned with the concrete blocks limit, without eccentricity. A notch was not inserted in Tanaka and Murakoshi (2011) specimens and that fact can justify the lower dowel strength values achieved. Moreover, the  $V_d-s$  relations for the Rasmussen (1963) and Tanaka and Murakoshi (2011) tests are not available. Force and displacement measurements are very important when the experimental calibration of a dowel action nonlinear FE model is intended.

For the reasons mentioned, and summarized in Table 2, Dei Poli *et al.* (1992) experimental program will be taken as a reference, in the following sections, for FE modeling of dowel action, considering a discrete representation. The test setup designed by Dei Poli *et al.* (1992) eliminated the main factors or mechanisms interfering with dowel behavior and strength: concrete splitting, aggregate interlock interaction, kinking effect of reinforcement and confinement induced by stirrups.

### 3. Definition of an empirical model

Since the aim of the present study is to develop a FE model that can be applied to a wide range of bar diameters and concrete strengths, it is necessary to have a way to predict dowel behavior for cases in which those parameters

are different from the ones in the experimental tests considered. In order to interpolate that behavior for several bar diameters and concrete strengths, an empirical model with a very good correlation to the experimental data available must be defined.

Several authors have proposed empirical models resulting from an adjustment to the values measured in their tests, namely: Dei Poli *et al.* (1992), Dulacska (1972), Millard and Johnson (1984), Vintzeleou and Tassios (1986) and Walraven and Reinhardt (1981). In view of the fact that Dei Poli *et al.* (1992) campaign will be taken as a reference, its empirical model will also serve as an interpolation tool of dowel behavior. In this context, Dei Poli *et al.* (1992) compared their proposal with the ones of Vintzeleou and Tassios (1986) and Walraven and Reinhardt (1981), pointing some differences. The model uses the following expression for the  $V_d-s$  relation that comes from the BEF analogy

$$V_d = 2 \times \alpha^3 \times E_s \times I \times s \quad (5)$$

in which

$$\alpha = \sqrt[4]{\frac{k_c \times \phi}{4 \times E_s \times I}} \quad (6)$$

where  $E_s$  is the steel Young modulus and  $I$  the reinforcement moment of inertia. In turn, stiffness  $k_c$  of the concrete substrate is the product of a nonlinearity coefficient  $\omega$  with elastic stiffness  $k_0$

$$k_c = \omega \times k_0 \quad (7)$$

with  $\omega$  and  $k_0$  given by

$$\omega(s, \phi, f_c) = \left[ 1.5 \times \left( a + \sqrt{d^2 \times \left( \frac{40 \times s}{\phi} - b \right)^2 + c^2} \right) \right]^{\frac{4}{3}} \quad (8)$$

$$k_0 = \frac{600 \times f_c^{0.7}}{\phi} \quad (9)$$

In Eqs. (7) to (9),  $f_c$  is in MPa,  $k_0$  in MPa/mm and  $\phi$  in mm. The four coefficients  $a$ ,  $b$ ,  $c$  and  $d$  are linear functions of the concrete strength. Nevertheless, the comparison between this empirical model and the Dei Poli *et al.* (1992) test data allowed to notice that an improvement could be made on stiffness  $k_0$  seeking a better fitting in terms of dowel behavior. Table 3 shows values obtained for Eq. (2) coefficient  $K$  considering the experimental results, the empirical model with stiffness  $k_0$  and the empirical model with a slightly changed stiffness  $k_{0^*}$

$$k_{0^*} = \frac{700 \times f_c^{0.7}}{\phi} \quad (10)$$

It can be seen that a very good fit is achieved when  $k_{0^*}$  is considered instead of  $k_0$ . The better fitting provided by  $k_{0^*}$  was not only observed for dowel strength values,  $V_{dR}$ , of Table 3, but also for the nonlinear  $V_d-s$  response (see Fig. 4 for  $f_c=32.3$  MPa). The  $V_{dR}$  value of the empirical model was calculated as the maximum dowel force predicted by Eq. (5) until  $s=s_{\max}$ .

Table 3 Comparison between Dei Poli *et al.* (1992) experimental results and its empirical model (with substrate stiffness given by  $k_0$  and  $k_{0^*}$ ) in terms of dowel resistance  $V_{dR}$

test	$\phi$ (mm)	$f_c$ (MPa)	experimental		empirical model - $k_0$		empirical model - $k_{0^*}$	
			$V_{dR}$ (kN)	$K$	$V_{dR}$ (kN)	$K$	$V_{dR}$ (kN)	$K$
A1	24	29.5	76.19	1.387	67.51	1.229	75.78	1.379
A2	24	29.5	80.00	1.456	67.51	1.229	75.78	1.379
A4	18	29.5	46.39	1.501	38.36	1.241	43.06	1.393
A6	18	29.5	49.42	1.599	38.36	1.241	43.06	1.393
A12	18	29.5	36.38	1.177	38.36	1.241	43.06	1.393
A13	18	29.5	45.09	1.459	38.36	1.241	43.06	1.393
A8	14	29.5	31.11	1.664	23.26	1.244	26.11	1.397
A9	14	29.5	27.24	1.457	23.26	1.244	26.11	1.397
A3	24	32.3	80.33	1.397	73.45	1.278	82.45	1.434
B1	24	32.3	84.08	1.462	73.45	1.278	82.45	1.434
B4	24	32.3	79.68	1.386	73.45	1.278	82.45	1.434
A10	18	32.3	46.25	1.430	41.65	1.288	46.76	1.446
B2	18	32.3	46.57	1.440	41.65	1.288	46.76	1.446
B5	18	32.3	43.46	1.344	41.65	1.288	46.76	1.446
B3	14	32.3	27.35	1.398	25.37	1.297	28.48	1.456
B6	14	32.3	27.02	1.381	25.37	1.297	28.48	1.456
E1	24	72.0	119.14	1.388	122.56	1.428	137.58	1.603
E2	18	72.0	75.96	1.573	68.94	1.428	77.39	1.603
E3	14	72.0	50.43	1.727	41.71	1.428	46.82	1.603
			$\mu$	1.454		1.289		1.447
			$\sigma$	0.123		0.066		0.074

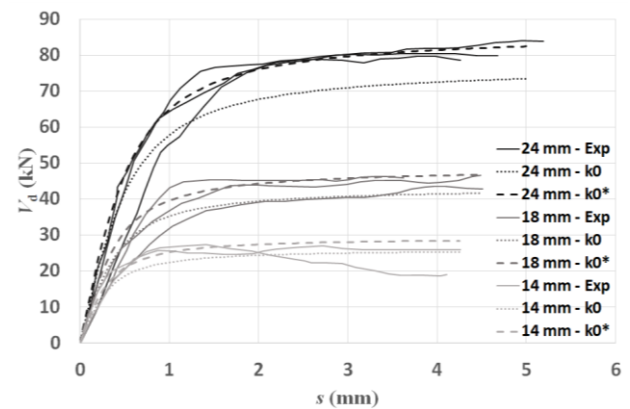


Fig. 4 Comparison of the empirical model results (having concrete substrate stiffness given by  $k_0$  and  $k_{0^*}$ ) with experimental values obtained by Dei Poli *et al.* (1992) ( $f_c=32.3$  MPa)

#### 4. Fixed Bed modeling approach

Different approaches to model dowel action are possible depending on the purpose of the analysis. If the purpose is the assessment of an isolated dowel, then a simpler approach is sufficient. This one is, in the present work, denoted by Fixed Bed (FB) approach. In this case, the concrete deformation is lumped in several interface spring elements which connect the steel bar to a fixed bed. These springs are designated in this paper by nonlinear Winkler springs.

#### 4.1 Finite element model description

The implemented FB modeling approach intends to characterize the dowel action mechanism of Fig. 1. The deformability of the concrete substrate under the reinforcing bar is modeled through a set of one-node translation nonlinear Winkler springs supported on a fixed bed. Every bar node is connected to one spring.

This FB model is a discrete representation of the dowel mechanism, composed by a single circular steel bar divided into 50 fully numerically integrated Mindlin beam (class-III) (DIANA 2014) FEs with shear deformation contemplated. Each element has a length of 8 mm, 3 nodes, 2 Gauss integration points along its axis and 24 over its cross-section. The cross-section is integrated with a 6-point Trapezium rule in the tangential direction and a 4-point Gauss scheme in the radial direction. The total length of the steel bar is 400 mm in order to match Dei Poli *et al.* (1992) specimen dimensions.

Five different bar diameters were considered (8, 12, 16, 20 and 25 mm), as well as 3 concrete strengths (29.5, 48.1 and 67.8 MPa), intending to cover a wide and recurrent range for these parameters. The first concrete strength value corresponds to the weaker concrete tested in Dei Poli *et al.* (1992) campaign, and the last two refer to old and new concretes of Figueira *et al.* (2015) specimens M1, M2 and M3.

Steel reinforcement material properties are the following: Young's modulus  $E_s=200$  GPa, Poisson's ratio  $\nu=0.3$ , yield stress  $f_y=605.4$  MPa and tensile strength  $f_t=631.8$  MPa. These strength values were determined in axial tests performed on reinforcing bar specimens, with specified characteristic yield stress of 500 MPa, made with the same steel that was used in specimens DM1, DM2 and DM3. To simulate steel yielding in the FE analyses, a Tresca maximum shear stress condition is adopted (Owen and Hinton 1980). Fig. 5 shows steel stress-strain ( $\sigma_s-\varepsilon_s$ ) relation assumed in the model, with initial linear-elastic behavior and post-yielding strain-hardening.

Since material plasticity is taken into account, the structural analysis involves the solution of a nonlinear analytical problem. Therefore, an iterative procedure is needed. In this work, the BFGS Quasi-Newton (Secant) method is used, with a Line Search algorithm to enhance the robustness of the iteration method (DIANA 2014). When the specified convergence criterion is satisfied, the calculation stops. In this context, an energy norm ratio is used for convergence criteria.

#### 4.2 Constitutive model for the nonlinear Winkler springs

##### 4.2.1 Procedure for calibration of the constitutive model

A procedure is adopted in the present study to set, or adjust, analytical expressions to describe the non-linear behavior of Winkler springs. In the FB modeling approach, all the Winkler springs along the bar length follow the same constitutive behavior. Experimental data from Dei Poli *et al.* (1992) and its empirical model with elastic stiffness  $k_{0*}$  are used to calibrate the adjustment. Since direct

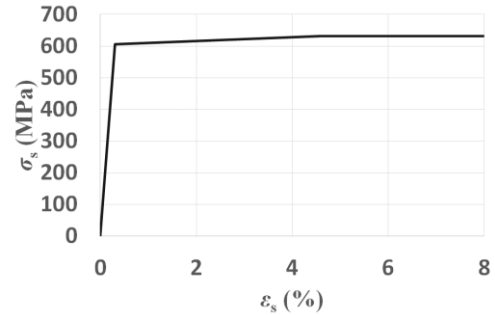


Fig. 5 Stress-strain rebar diagram considered in FE analyses

determination of those expressions is not possible, an iterative trial-error method was carried out. A mathematical formulation of the spring response is firstly conceived, and then the approximation between the FE results and the results provided by the empirical model is checked. This procedure aims to reach a balance between the ideal fit to the empirical model and a simple analytical representation of spring force-displacement relation. This procedure can be seen as a retro-analysis methodology.

In the procedure, the dowel force  $V_d$  is calculated as the sum of all spring vertical forces  $F_v$  in the model

$$V_d = \sum_{i=1}^n F_{v,i} \quad (11)$$

with

$$dF_v = k_{sp} \times d\delta_v \quad (12)$$

In turn, the spring stiffness  $k_{sp}$  is given by

$$k_{sp} = \psi(\delta_v, \phi, f_c) \times k_{0*} \quad (13)$$

where  $\psi$  is a nonlinearity coefficient and the elastic stiffness  $k_{0*}$  is given in Eq. (10).

Therefore, the analytical representation of spring behavior will provide the mathematical expressions for the coefficient  $\psi$ , depending on the diameter of the steel bar and on the material properties of concrete.

In the following subsection the analytical formulation adopted for the spring constitutive model is explained. Then, the derivation of the values of the various model parameters is presented.

##### 4.2.2 Analytical representation of spring behavior

Different possibilities for the nonlinear Winkler spring response were tested. It was concluded that the incremental force-displacement relation of Eq. (12) can be expressed through five different stages (see Fig. 6): I–initial linear elastic branch; II–nonlinear branch with increasing force; III–nonlinear branch with decreasing force; IV–smooth linear branch; V–constant residual branch.

Stages I to III resemble the typical stress-strain relation of concrete subjected to uniaxial compression, where the nonlinear response of stage II is caused by microcracking (Hsu *et al.* 1963), and the strength decrease of stage III by a vertical crack (Soroshian *et al.* 1987) appearing right below and along the reinforcing bar axis. The vertical crack seems to be much more pronounced in dowels embedded on

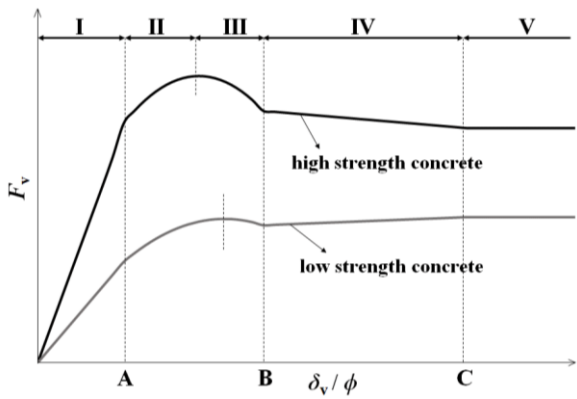


Fig. 6 Stages in the constitutive model for nonlinear Winkler springs

high strength concrete, whose model results point to an abrupt decrease in spring force  $F_v$ .

Stage IV discloses an increment in spring stiffness  $k_{sp}$ , until a residual strength is reached in stage V. This type of behavior is due to the fact that the concrete under the steel bar is subjected to a concentrated load. Therefore, the lateral dilatancy of the locally compressed concrete is hindered by the surrounding mass of non-loaded concrete, which results in a biaxial or triaxial stress state (Mander *et al.* 1988). In models with the lowest concrete strength considered ( $f_c=29.5$  MPa), an increase in spring force during stage IV is also observed, showing that the propagation of the vertical crack below the reinforcing bar is more gradual in these cases.

The analyses revealed that a single quadratic function could be used to describe the  $F_v-\delta_v$  relation in stages II and III (see Fig. 6). Therefore, in these stages, the parameter  $\psi$  is a linear function of the string displacement  $\delta_v$ . It was also concluded that a satisfying adjustment is reached if a linear branch is adopted for stage IV. These conclusions are resumed in the subsequent expressions for coefficient  $\psi$

$$\psi_I = a \ll \frac{\delta_v}{\phi} < A \quad (14)$$

$$\psi_{II,III} = b \times \left( \frac{\delta_v}{\phi} \right) + c \ll A \leq \frac{\delta_v}{\phi} \leq B \quad (15)$$

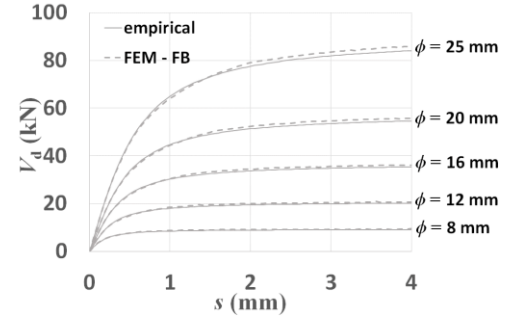
$$\psi_{IV} = d \ll B < \frac{\delta_v}{\phi} < C \quad (16)$$

$$\psi_V = 0 \ll \frac{\delta_v}{\phi} \geq C \quad (17)$$

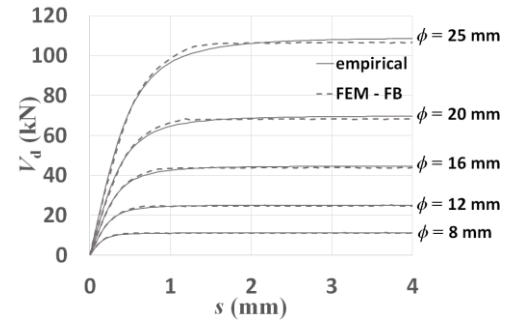
in which  $A$ ,  $B$  and  $C$  coefficients mark the transition between stages, as shown in Fig. 6. Therefore, the values of  $\delta_v$  at those instants depend on the reinforcing bar diameter. The influence of concrete strength is accounted for on coefficients  $a$ ,  $b$ ,  $c$  and  $d$ .

#### 4.2.3 Determination of the spring model coefficients for the FB approach

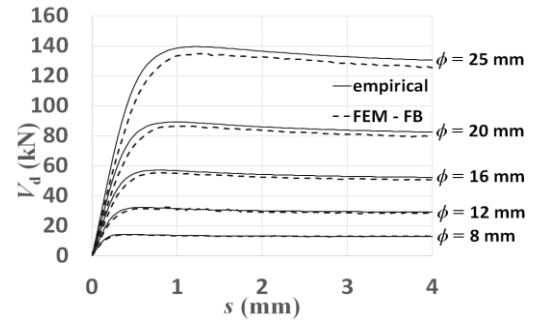
The constitutive model for nonlinear Winkler springs



(a)



(b)



(c)

Fig. 7 Comparison of dowel force values obtained through the empirical model and FE model for the Fixed Bed (FB) approach: (a)  $f_c=29.5$  MPa; (b)  $f_c=48.1$  MPa; (c)  $f_c=67.8$  MPa

becomes completely defined once the coefficients  $A$ ,  $B$  and  $C$  and also  $a$ ,  $b$ ,  $c$  and  $d$  are determined. In order to obtain these coefficients, the retro-analysis methodology explained in section 4.2.1 was performed for each different combination of bar diameter and concrete strength. Therefore, 15 retro-analyses were made (3 concretes times 5 diameters). It was concluded that fixed values could be adopted for the coefficients  $A$ ,  $B$  and  $C$  of Eq. (14) to (17):

$$A = 0.0065$$

$$B = 0.022$$

$$C = 0.117$$

These coefficient values are thus independent from the bar diameter and the concrete strength. On the other hand, the coefficients  $a$ ,  $b$ ,  $c$  and  $d$  to be used in the FB modeling approach can be expressed by the following linear functions of the concrete strength

$$a = 0.0116 \times f_c + 0.4261 \quad (18)$$

$$b = -1.068 \times f_c - 13 \quad (19)$$

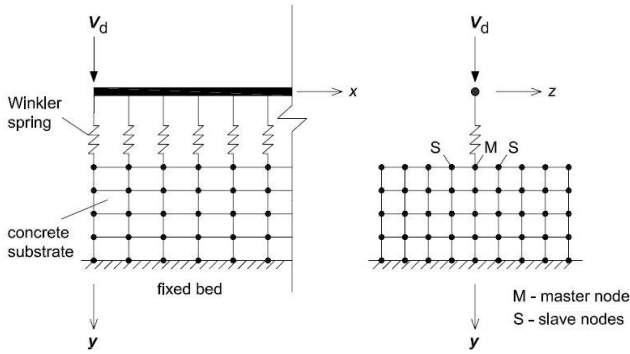


Fig. 8 Embedded Dowel (ED) FE model for dowel action analyses

$$c = 0.02275 \times f_c + 0.267 \quad (20)$$

$$d = -0.00184 \times f_c + 0.0825 \quad (21)$$

with  $f_c$  in MPa. These expressions are valid for any bar diameter and concrete strength within the upper and lower bounds considered in this work (indicated before):  $29.5 \text{ MPa} \leq f_c \leq 67.8 \text{ MPa}$  and  $8 \text{ mm} \leq \phi \leq 25 \text{ mm}$ . It should be noted that, in the empirical model proposed by Dei Poli *et al.* (1992), the parameters which characterize the dowel response (Eq. (8)) are also linear functions of the concrete strength. Therefore, the shape of the previous Eqs. (18) to (21) is not surprising.

Fig. 7 shows the comparison between the results provided by the empirical model and the outcome of FE analysis (according to the FB approach), considering the constitutive model for the springs defined before (Eqs. (14) to (21)). A very good fit can be seen for the 3 concrete strengths and 5 bar diameters considered.

## 5. Embedded Dowel modeling approach

The Fixed Bed modeling approach cannot be implemented in the analysis of a real structure discretized with solid brick FEs, or plane stress elements. In those cases, the nonlinear Winkler springs are not connected to a rigid element. Instead, they are connected to the deformable solid brick or plane stress FEs. Therefore, a so-called Embedded Dowel (ED) approach is also envisaged in this work. In the example shown below, the concrete substrate is discretized through solid brick elements; however the analysis approach can be applied to structures in which the concrete medium is discretized with plane stress elements without loss of generality.

### 5.1 Finite element model description

The ED model is illustrated in Fig. 8. The concrete substrate block has linear elastic behavior. Nonlinearity is accounted for in reinforcement and springs only. In the ED model, interface springs are two-node translation elements which link the steel bar to concrete in the vertical direction only ( $y$  direction in Fig. 8). The connected bar and substrate nodes are coincident. In the schematic representation of Fig.

8 they are not coincident just to make the drawing clear.

In the horizontal  $x$  direction, the bar and substrate nodes would have to be connected (though a horizontal nonlinear spring) if the bar was subjected to axial force. No axial force is applied to the bar in this example and, for that reason, steel and substrate nodes are not connected in the  $x$  direction, except in one bar node to avoid instability of the FE model.

The bar is not loaded in the horizontal  $z$  direction. Therefore, bar and substrate displacements are equal in the horizontal  $z$  direction.

In this ED approach, each spring links one bar node to a single concrete substrate master node, which then connects to neighboring slave nodes in the transverse  $z$  direction, as can be seen in Fig. 8, through tying conditions included in the model. These tyings impose that the vertical displacement of slave nodes is equal to the displacement of their master node. In turn, the number of slave nodes in each transverse alignment depends on the bar diameter. That number is increased for larger bar diameters in order to get a more realistic load distribution under the reinforcing bar.

### 5.2 Derivation of the constitutive model for the nonlinear Winkler springs

In the ED approach, the constitutive model for the nonlinear Winkler springs depends on the discretization and characteristics of the concrete substrate. In order to take account of this issue, a procedure is proposed in the following paragraphs, to determine the spring constitutive model for an ED modeling approach.

The procedure is based on the fact that Eqs. (14) to (21) give the expressions for the approach with fixed bed (the so-called FB approach), which can be taken as a reference for the definition of the constitutive model in the ED approach. Then, it is important to note that, in the ED approach, the reinforcing bar is supported by a system which can be seen as an association in series of a spring and the concrete substrate FEs. Therefore, the deformation of the spring with fixed bed, given by Eqs. (14) to (21), has to be equal to the deformation of this association in series. The relationship between the stiffness of a spring in the FB approach,  $k_{sp,FB}$ , and the corresponding sum of stiffnesses of all springs connecting to a certain bar node in the ED approach,  $k_{sp,ED}$ , is given by Eq. (22)

$$\frac{1}{k_{sp,FB}} = \frac{1}{k_{sp,ED}} + \frac{1}{k_{sub}} \quad (22)$$

As the constitutive relations for the springs are nonlinear,  $k_{sp,FB}$  and  $k_{sp,ED}$  are tangent stiffnesses. On the contrary,  $k_{sub}$  is the elastic stiffness of the concrete substrate and has a constant value. Thus, to determine in a simple way the values of  $k_{sp,ED}$  through Eq. (22), the constitutive model of the FB approach springs is written as a multilinear function. Moreover, it is necessary to know the value of  $k_{sub}$  for the FE model conceived. For that purpose, the following steps should be taken:

- 1 – Determination of the displacements  $\delta_v$ , throughout the length of the steel bar, for a certain slip ( $s$ ) value in

Table 4 Number of slave nodes in the transverse  $z$  direction and its spacing for each bar diameter, in the ED modeling approach

$\phi$ (mm)	$s_{sp}$ (mm)	$N$
8	4	2
12	5	2
16	4	4
20	5	4
25	4	6

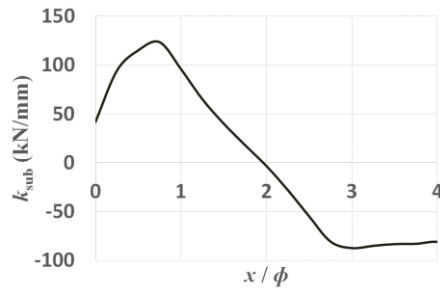


Fig. 9 Elastic stiffness  $k_{sub}$  of concrete substrate in an ED model with  $f_c=48.1$  MPa and  $\phi=16$  mm ( $s_{sn}=4$  mm from Table 4 and  $x$  axis identified in Fig. 1 and Fig. 8)

the FB FE model.

2 – Imposition of the displacement profile determined in the previous step to the steel bar of the ED FEM model. In this phase, the constitutive relations of the FB approach are assigned to the springs of the ED FE model. In order to impose displacements, vertical supports need to be added to the bar nodes, in the ED FE model.

3 – Calculation of the reactions  $F_v$  in the ED model and the corresponding stiffness  $k_{sub}=F_v/\delta_{v,sub}$ , in which  $\delta_{v,sub}$  is the vertical ( $y$  direction in Fig. 8) displacement of the concrete substrate.

### 5.3 Example

In this section, an example of dowel behavior assessment through the ED modeling approach is described. A model similar to the one presented in Fig. 8 is assumed, with concrete substrate modeled through eight node isoparametric solid brick elements and an 8-point ( $2 \times 2 \times 2$ ) Gauss integration scheme. The concrete block is 400 mm long, 192 mm high and 240 mm wide, matching Dei Poli *et al.* (1992) specimens. This block is supported on a fixed bed. The solid brick elements used in the block discretization are 4 mm long and 4 mm high. Their width depends on the bar diameter. In this context, Table 4 shows the number of slave nodes  $N$  in the transverse  $z$  direction, and its spacing  $s_{sn}$  considered for each bar diameter.

The concrete material properties considered are Poisson ratio  $\nu=0.2$  and Young's modulus  $E_c$  calculated through the *fib* Model Code (*fib* 2013) expression  $E_c=21500 \times (f_c/10)^{1/3}$  with  $E_c$  and  $f_c$  in MPa. For the steel properties, the values used in the FB approach are maintained. In turn, the connection between the steel bar and the concrete substrate

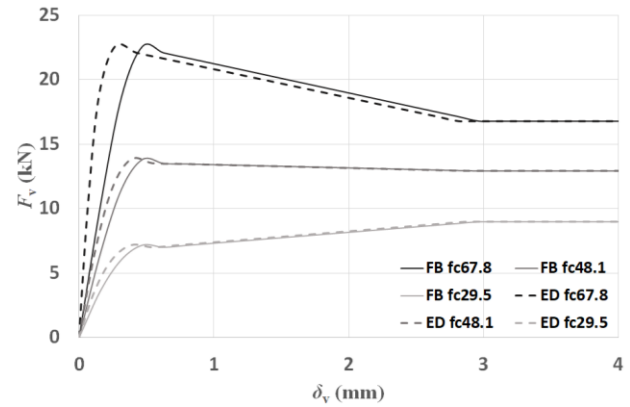


Fig. 10 Winkler spring force results achieved in the FE models with  $\phi = 25$  mm

is established through Winkler springs, whose constitutive relations are calculated using Eq. (22) and the explained procedure for  $k_{sub}$  determination.

Fig. 9 displays the  $k_{sub}$  values obtained for a model with  $f_c=48.1$  MPa and  $\phi=16$  mm ( $s_{sn}=4$  mm from Table 4). It can be seen that the stiffness has a minimum at the specimen theoretical “crack” section ( $x=0$  mm), rapidly increases near the “crack”, and then gradually decreases until reaching negative values at  $x/\phi=2$ , when the deformation  $\delta_v$  of the steel bar starts to have negative values.

Theoretically, since  $k_{sub}$  varies along the steel bar  $x$  axis, different constitutive models have to be determined through Eq. (22) for the nonlinear Winkler springs of the ED approach. However, very good results can be achieved, with an almost identical dowel response between the ED and the FB approaches, if only two values for  $k_{sub}$  are considered: one value  $k_{sub1}=k_{sub}$  ( $x=0$ ) for the first spring at the “crack” section, and a second value  $k_{sub2}$  for the remaining springs. For  $k_{sub2}$ , it is recommended the average value of  $k_{sub}$  calculated for nodes located between  $0 < x < \phi$ .

Fig. 10 depicts the obtained constitutive models for the springs, given by Eqs. (14) to (22). The figure shows the models for a bar diameter  $\phi=25$  mm and for the three concrete strengths considered in this work. These curves correspond to the constitutive behavior which is represented in Fig. 6. It can be seen in Fig. 10 that the constitutive model to be used in ED models has to have a higher stiffness in the first ascending branch, compared to the stiffness in FB models. This is the result of the condition imposed by Eq. (22). For greater displacement values, the constitutive model for the ED approach is almost coincident with the one of the FB approach.

## 6. Conclusions

A nonlinear FE modeling approach was developed to assess the behavior of a dowel steel bar embedded on a concrete block, subjected to monotonic loading. In the approach, a discrete representation is considered, in which the reinforcing bar is connected to the concrete embedment through nonlinear Winkler spring elements. Then, the constitutive relations for the springs were achieved through

the comparison between the FE model outcomes and the available experimental results for dowel action. The main conclusions that can be derived from the work in this paper are the following:

- Experimental assessment of reinforcing bar dowel action in a concrete interface is a complex task. The conception of a specimen execution procedure that can eliminate interface roughness is hard to accomplish and, consequently, the probability of dowel action interacting with aggregate interlock as an interface strength mechanism is significant. Moreover, reinforcement kinking effect arises in concrete interfaces for large slip values, also contributing for shear strength. The recommended procedure is the evaluation of dowel action in a single concrete block, removing the input of other strength mechanisms.
- In order to calibrate a finite element model for dowel action that can be applied to a wide range of bar diameters and concrete strengths, the Dei Poli *et al.* (1992) empirical model was considered. Comparing the model with the tests performed by Dei Poli *et al.* (1992), it was concluded that a slight change in the proposed stiffness for concrete substrate results in an important improvement in the adjustment to the experimental results.
- The FE model conceived contains a complete discrete “beam element” representation of the steel reinforcing bar, accounting for flexural stiffness and nonlinear material behavior. The bar is connected to concrete embedment through discrete Winkler spring elements, with nonlinear constitutive relations, to simulate the deformability and strength of the concrete substrate. Two different approaches were proposed: 1—a Fixed Bed approach, suitable for an isolated analysis of dowel action, in which the concrete deformability is totally lumped in the nonlinear Winkler springs; 2—an Embedded Dowel approach, suitable for simulation of dowel action in structures (or parts of structures) modeled with solid brick or plane stress finite elements.
- The constitutive model for the nonlinear Winkler springs was defined and calibrated. In the case of the fixed bed modeling approach, this model is given by closed form expressions, valid for a wide and recurrent range of values for bar diameter and concrete strength. In the case of the embedded dowel approach, a modified constitutive model has to be employed. The procedure for definition of such model was also shown in the paper.

## Acknowledgments

This work was financially supported by: Project POCI-01-0145-FEDER-007457-CONSTRUCT-Institute of R&D in Structures and Construction funded by FEDER funds through COMPETE2020-Programa Operacional Competitividade e Internacionalização (POCI) and by national funds through FCT-Fundação para a Ciência e a Tecnologia; PhD Grant SFRH/BD/65111/2009. The support provided by LEMC-Laboratório de Ensaio de Materiais de Construção is also gratefully acknowledged.

## References

- Bennett, E.W. and Banerjee, S. (1976), “Strength of beam-column connections with dowel reinforcement”, *Struct. Eng.*, **54**(4), 133-139.
- Davids, W.G. and Turkiyyah, G.M. (1997), “Development of embedded bending member to model dowel action”, *J. Struct. Eng.*, ASCE, **123**(10), 1312-1320.
- Dei Poli, S., Di Prisco, M. and Gambarova, P.G. (1992), “Shear response, deformations, and subgrade stiffness of a dowel bar embedded in concrete”, *ACI Struct. J.*, **89**(6), 665-675.
- DIANA (2014), DIANA Finite Element Analysis User’s Manual Release 9.6, TNO DIANA BV, Delft, The Netherlands.
- Dias-da-Costa, D., Alfaiate, J. and Júlio, E.N.B.S. (2012), “FE modeling of the interfacial behaviour of composite concrete members”, *Constr. Build. Mater.*, **26**, 233-243.
- Dulacska, H. (1972), “Dowel action of reinforcement crossing cracks in concrete”, *ACI J. Proc.*, **69**(12), 754-757.
- Engström, B. (1990), “Combined effect of dowel action and friction in bolted connections”, *Nordic Concrete Res.*, **9**, 14-33.
- fib-fédération internationale du béton (2008), Structural connections for precast concrete buildings, fib Bulletin 43, Lausanne, Switzerland.
- fib-fédération internationale du béton (2013), fib Model Code for concrete structures 2010, Ernst & Sohn Publisher, Berlin, Germany.
- Figueira, D., Sousa, C., Calçada, R. and Serra Neves, A. (2015), “Push-off tests in the study of cyclic behavior of interfaces between concretes cast at different times”, *J. Struct. Eng.*, ASCE, **142**(1), 04015101.
- Friberg, B.F. (1938), “Design of dowels in transverse joints of concrete pavements”, *Proc. Am. Soc. Civil Eng.*, **64**(9), 1809-1828.
- Guo, H., Sherwood, J.A. and Snyder, M.B. (1995), “Component dowel-bar model for load-transfer systems in PCC pavements”, *J. Tran. Eng.*, ASCE, **121**(3), 289-298.
- He, X.G. and Kwan, A.K.H. (2001), “Modeling dowel action of reinforcement bars for finite element analysis of concrete structures”, *Comput. Struct.*, **79**, 595-604.
- Hsu, T.T., Slate, F.O., Sturman, G.M. and Winter, G. (1963), “Microcracking of plain concrete and the shape of the stress-strain curve”, *ACI J. Proc.*, **60**(2), 209-224.
- Kazaz, I. (2011), “Finite element analysis of shear-critical reinforced concrete walls”, *Comput. Struct.*, **8**(2), 143-162.
- Kwan, A.K.H. and Ng, P.L. (2013), “Modeling dowel action of discrete reinforcing bars for finite element analysis of concrete structures”, *Comput. Concrete*, **12**(1), 19-36.
- Mackiewicz, P. (2015), “Finite-element analysis of stress concentration around dowel bars in jointed plain concrete pavement”, *J. Tran. Eng.*, **141**(6), 06015001.
- Maekawa, K. and Qureshi, J. (1996), “Computational model for reinforcing bar embedded in concrete under combined axial pullout and transverse displacement”, *J. Mater. Concrete Struct. Pave.*, *JPN Soc. Civil Eng.*, **31**(538), 227-239.
- Maekawa, K. and Qureshi, J. (1997), “Stress across interfaces in reinforced concrete due to aggregate interlock and dowel action”, *J. Mater. Concrete Struct. Pave.*, *JPN Soc. Civil Eng.*, **34**(557), 159-172.
- Magliulo, G., Ercolino, M., Cimmino, M., Capozzi, V. and Manfredi, G. (2014), “FEM analysis of the strength of RC beam-to-column dowel connections under monotonic actions”, *Constr. Build. Mater.*, **69**, 271-284.
- Mander, J.B., Priestley, M.J. and Park, R. (1988), “Theoretical stress-strain model for confined concrete”, *J. Struct. Eng.*, ASCE, **114**(8), 1804-1826.
- Millard, S.G. and Johnson, R.P. (1984), “Shear transfer across cracks in reinforced concrete due to aggregate interlock and to

- dowel action”, *Mag. Concrete Res.*, **36**(126), 9-21.
- Moradi, A.R., Soltani, M. and Tasnimi, A.A. (2012), “A simplified constitutive model for dowel action across RC cracks”, *J. Adv. Concrete Technol.*, **10**, 264-277.
- Owen, D.R.J. and Hinton, E. (1980), *Finite Elements in Plasticity: Theory and Practice*, 1<sup>st</sup> Edition, Pineridge Press Limited Publisher, Swansea, United Kingdom.
- Paulay, T., Park, R. and Phillips, M.H. (1974), “Horizontal construction joints in cast-in-place reinforced concrete”, *ACI Spec. Publ.*, **42**(27), 599-616.
- Pimentel, M., Cachim, P. and Figueiras, J. (2008), “Deep-beams with indirect supports: numerical modeling and experimental assessment”, *Comput. Concrete*, **5**(2), 117-134.
- Rahal, K.N., Khaleefi, A.L. and Al-Sanee, A. (2016), “An experimental investigation of shear-transfer strength of normal and high strength self compacting concrete”, *Eng. Struct.*, **109**, 16-25.
- Randl, N. (1997), “Untersuchungen zur Kraftübertragung zwischen Alt- und Neubeton bei unterschiedlichen Fugenhöhigkeiten”, Ph.D. Dissertation, Universität Innsbruck, Innsbruck.
- Randl, N. (2013), “Design recommendations for interface shear transfer in fib Model Code 2010”, *Struct. Concrete*, **14**(3), 230-241.
- Rasmussen, B.H. (1963), “The carrying capacity of transversely loaded bolts and dowels embedded in concrete”, *Bygningsstatistiske Meddelelser*, **34**(2), 39-55.
- Santos, P.M.D. and Júlio, E.N.B.S. (2014), “Interface shear transfer on composite concrete members”, *ACI Struct. J.*, **111**(1), 113-121.
- Soroushian, P., Obaseki, K. and Rojas, M.C. (1987), “Bearing strength and stiffness of concrete under reinforcing bars”, *ACI Mater. J.*, **84**(3), 179-184.
- Soroushian, P., Obaseki, K., Rojas, M.C. and Sim, J. (1986), “Analysis of dowel bars acting against concrete core”, *ACI J. Proc.*, **83**(4), 642-649.
- Tanaka, Y. and Murakoshi, J. (2011), “Reexamination of dowel behavior of steel bars embedded in concrete”, *ACI Struct. J.*, **108**(6), 659-668.
- Tsoukantas, S.G. and Tassios, T.P. (1989), “Shear resistance of connections between reinforced concrete linear precast elements”, *ACI Struct. J.*, **86**(3), 242-249.
- Vintzeleou, E.N. and Tassios, T.P. (1986), “Mathematical models for dowel action under monotonic and cyclic conditions”, *Mag. Concrete Res.*, **38**(134), 13-22.
- Vintzeleou, E.N. and Tassios, T.P. (1987), “Behavior of dowels under cyclic deformations”, *ACI Struct. J.*, **84**(3), 18-30.
- Walraven, J.C. and Reinhardt, H.W. (1981), “Theory and experiments on the mechanical behavior of cracks in plain and reinforced concrete subjected to shear loading”, *Heron*, **26**(1A).
- Zoubek, B., Fahjan, Y., Fischinger, M., and Isaković, T. (2014), “Nonlinear finite element modelling of centric dowel connections in precast buildings”, *Comput. Concrete*, **14**(4), 463-477.